Assessment and validation of the MS/MS fragmentation patterns of the macrolide immunosuppressant everolimus

8 AUTHORS, INCLUDING:

Wolfgang Jacobsen
Oslo University Hospital
73 PUBLICATIONS   2,429 CITATIONS

SEE PROFILE

Tobin Strom
Moffitt Cancer Center
59 PUBLICATIONS   182 CITATIONS

SEE PROFILE

Frank Streit
Universitätsmedizin Göttingen
42 PUBLICATIONS   1,036 CITATIONS

SEE PROFILE

Uwe Christians
University of Colorado
162 PUBLICATIONS   4,139 CITATIONS

SEE PROFILE

JMS

Assessment and validation of the MS/MS fragmentation patterns of the macrolide immunosuppressant everolimus

K. Olaf Boernsen,[1] Wolfgang Egge-Jacobsen,[2][†] Bruno Inverardi,[3] Tobin Strom,[4] Frank Streit,[5] Hans-Martin Schiebel,[6] Leslie Z. Benet[7] and Uwe Christians[4]*

[1] Biomarker Development, Novartis Pharma AG, Basel, Switzerland
[2] Department of Molecular Biosciences, University of Oslo, Oslo, Norway
[3] Novartis Institutes for Biomedical Research, Basel, Switzerland
[4] Clinical Research and Development, Department of Anesthesiology, University of Colorado at Denver and Health Sciences Center, Denver, Colorado, USA
[5] Abteilung Klinische Chemie, Georg-August Universität, Göttingen, Germany
[6] Institut für Chemie, Technische Universität Braunschweig, Braunschweig, Germany
[7] Department of Biopharmaceutical Sciences, University of California, San Francisco, California, USA

Everolimus (40-*O*-(2-hydroxyethyl)rapamycin, Certican) is a 31-membered macrolide lactone. In lymphocytes, it inhibits the mammalian target of rapamycin (mTOR) and is used as an immunosuppressant after organ transplantation. Due to its instability in pure organic solvents and insufficient HPLC separation, NMR spectroscopy analysis of its metabolite structures is nearly impossible. Therefore, structural identification based on tandem mass spectrometry (MS/MS) and MS^n fragmentation patterns is critical. Here, we have systematically assessed the fragmentation pattern of everolimus during liquid chromatography (LC)-electrospray ionization (ESI)-MS/MS and validated the fragment structures by (1) comparison with structurally identified derivatives (sirolimus), (2) high-resolution mass spectrometry, (3) elucidation of fragmentation pathways using ion trap mass spectrometry (up to MS^5) and (4) H/D exchange. In comparison with the structurally related immunosuppressants tacrolimus and sirolimus, our study was complicated by the low ionization efficiency of everolimus. Detection of positive ions gave the best sensitivity, and everolimus and its fragments were mainly detected as sodium adducts. LC-ESI-MS/MS of everolimus in combination with collision-induced dissociation (CID) resulted in a complex fragmentation pattern and the structures of 53 fragments were identified. These detailed fragmentation pathways of everolimus provided the basis for structural elucidation of all everolimus metabolites generated *in vivo* und *in vitro*. Copyright © 2007 John Wiley & Sons, Ltd.

Supplementary electronic material for this paper is available in Wiley InterScience at http://www.interscience.wiley.com/jpages/1076-5174/suppmat/

INTRODUCTION

Everolimus (SDZ-RAD, Certican^R, Novartis Pharma AG, Basel, Switzerland,) is a 31-membered macrolide lactone: a semi-synthetic derivative of the macrolide immunosuppressant, sirolimus, 40-*O*-(2-hydroxyethyl)rapamycin, $C_{53}H_{83}NO_{14}$, molecular mass 957.5814 Da; (Fig. 1).[1] It has been demonstrated that everolimus is a potent immunosuppressant in solid organ transplant and autoimmune disease

models, and it inhibits proliferation of vascular smooth muscle cells.[2,3] The molecular mechanism underlying its immunosuppressive activity is similar to that of sirolimus.[4] Everolimus has successfully been used in combination with cyclosporine as rejection prophylaxis in transplant patients.[5] Everolimus is soluble in alcohols, acetonitrile, ethers, and halogenated hydrocarbons, and nearly insoluble in water and aliphatic hydrocarbons. Despite this, everolimus is unstable in pure organic solvents and, therefore, NMR spectroscopic analysis of its metabolites has been unsuccessful. Also, as shown *in vivo* and after incubation with microsomes *in vitro*, everolimus is metabolized to more than 20 metabolites. Because of this, only incomplete HPLC separation of its metabolites could be achieved and the purity of the isolated metabolite fractions would have been insufficient for NMR spectroscopic analysis. Electrospray ionization (ESI)-tandem

*Correspondence to: Uwe Christians, Clinical Research and Development, Department of Anesthesiology, University of Colorado at Denver and Health Sciences Center, 4200 East Ninth Ave., Room UH-2122, Denver, Colorado 80262, USA.
E-mail: uwe.christians@uchsc.edu
†W.E-J. and U.C. carried out most of their work described herein in L.Z.B.'s laboratory in the Department of Biopharmaceutical Sciences, University of California, San Francisco, California, USA

WILEY InterScience®
DISCOVER SOMETHING GREAT

mass spectrometry (MS/MS) has previously been used to identify the structures of several metabolites of the related sirolimus;[6-9] however, no attempt was made to further validate the hypothetical fragment structures. It is obvious from these publications that alternative structures for several fragments were possible. It was our goal to systematically assess the MS/MS fragmentation patterns of everolimus and to validate the fragment structures by (1) comparison with structurally identified derivatives (sirolimus), (2) high-resolution mass spectrometry, (3) elucidation of the fragmentation pathways using ion trap mass spectrometry (up to MS[5]) and (4) H/D exchange prior to everolimus fragmentation. These detailed fragmentation pathways of everolimus are the basis for further structural elucidation of metabolites produced *in vitro* and *in vivo*. These metabolite structures will be discussed in a separate paper, because of the high number and complexity of the different biotransformation products. The described HPLC system was originally developed for the separation of everolimus metabolites from human and animal *in vitro* and *in vivo* studies. However, in this study, it is only used to introduce pure compounds into the mass spectrometers and to perform H/D exchange experiments.

EXPERIMENTAL

Chemicals

All chemicals and organic solvents were of analytical or spectroscopic grade and were purchased from Fluka (Buchs, Switzerland). Deuterium oxide and deuterated methanol were from Cambridge Isotope Laboratories (Andover, Massachusetts). For confirmation of everolimus fragment structures, sirolimus was included in our study. Everolimus ($C_{53}H_{83}NO_{14}$, 958.22 Da), sirolimus ($C_{51}H_{79}NO_{13}$, 914.18 Da) and their derivatives were obtained from Transplantation Research, Novartis Pharma AG, Basel; laboratory grade (98% purity for analytical use). In addition, the precursor of seco acid of everolimus (PSA), with the molecular formula

$C_{53}H_{85}NO_{15}$ and exact mass 975.5915 Da, and the corresponding seco acid (SA) of everolimus, with the molecular formula $C_{53}H_{83}NO_{14}$ and exact mass of 957.5814 Da, were used as structurally identified reference compounds.

Everolimus and the other structurally related study compounds were found to nonspecifically bind to glass and plastic container walls to a statistically significant extent within 3 h. Adsorption was irreversible. To overcome this problem, only freshly prepared samples and silanized tubes and glassware were used. Stock solutions were prepared in acetonitrile/0.1% formic acid (4/1, v/v).

Chromatography

The HPLC system was based on a binary Agilent series 1100 pump (Agilent Technologies, Palo Alto, USA). To reduce the dead volume, the pump was modified, so that flow rates between 50 and 100 µl/min were achievable. An autosampler, model HTS-PAL (CTC Analytics, Zwingen, Switzerland), was used for sample injection and online solid phase extraction. The flow from the analytical column was split 1 : 5 into the MS and into a diode array detector with a 1 µl flow cell (Agilent Technologies, Palo Alto, USA).

HPLC separation was carried out on a 150 × 1 mm Xterra C18 column filled with 3 µm particles (Waters Milford, MA, USA). The samples were directly injected onto a 2 × 3 mm C8 cartridge used as sample trap column (Security Guard, Phenomenex, Torrance, CA, USA) using the syringe of the autosampler. Before sample injection, the cartridge was slowly conditioned with 100 µl water and 5% methanol, also supplied by the syringe of the autosampler. After the sample was trapped, the cartridge was rinsed with 100 µl pure water. The sample was then eluted in the forward-flush mode onto the analytical column (flow rate: 60 µl/min). The temperature of the column was set to 60 °C. The sample components were then separated by running a gradient using the following solvents A: 70% water + 10 mmol/l ammonium acetate adjusted to pH 7 and B: methanol. The following gradient was used: 0 min, 30% methanol; 26 min, 95% methanol; 30 min, 95% methanol. The column was re equilibrated to the starting conditions in 16 min. The total analysis time was 46 min. Peak half-widths were 9 s or less.

LC-MS/MS

All high mass resolution experiments were carried out on a quadrupole time-of-flight mass spectrometer (QTOF I; Micromass, Manchester, UK). The ESI was operated using nitrogen as the desolvation and nebulizing gas at a temperature of 150 °C. The spray capillary and the cone voltages were set to 2650 and 100 V, respectively. The cone block was heated to 120 °C and was set to a potential between 80 and 100 V. For CID experiments, argon was used as the collision gas and the collision energy was set to 55 V. The internal lock-mass for accurate determination of the molecular mass of the ions and their elemental composition was $C_{27}H_{45}NO_{7}Na^{+}$ (518.3094), a major everolimus fragment (Table 2 and Fig. 4). MS[3] experiments on the QTOF were carried out by insource CID followed by MS/MS analysis. For the correction of the TDC deadtime, the Masslynx function was used.
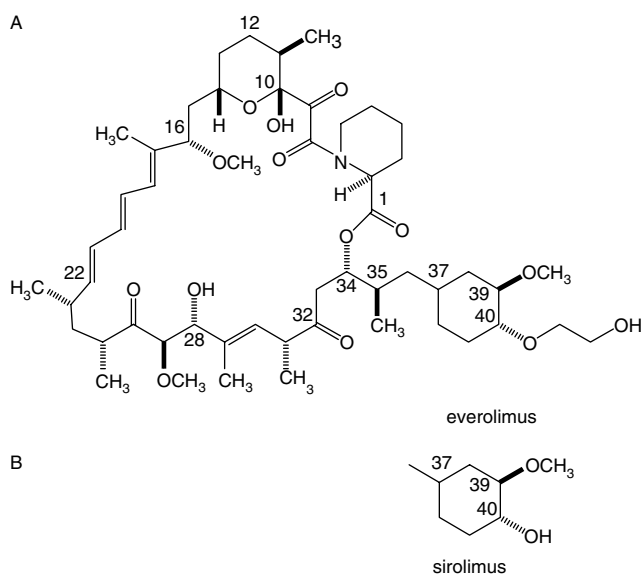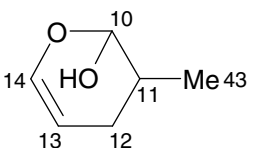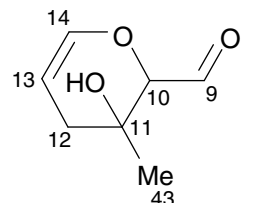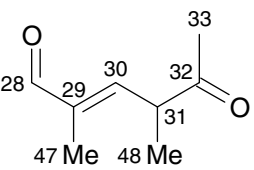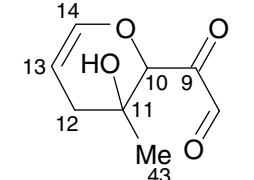

Figure 1. Structure of everolimus (40-*O*-(2-hydroxyethyl)rapamycin). Numbering of the C-atoms is as per the IUPAC guidelines[10].

Table 1. Key small neutral ass losses from everolimus and their combinations, Only observed masses are added in the table

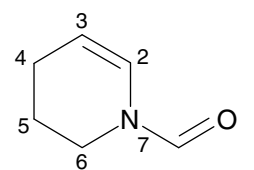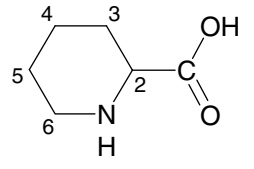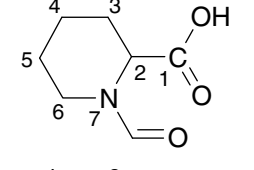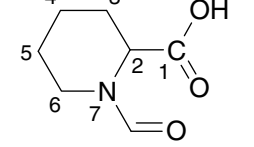| Neutral losses			h	w	l	x	m	k	mw	fxwe	fmw
	Mass differences		2	18	26	28	32	44	50	46	96
h:	H_2	2	–	–	28	30	–	46	–	–	–
w:	H_2O	18	–	–	–	46	50	–	–	–	–
l:	$HC{\equiv}CH$	26	28	–	–	–	–	–	76	–	–
c2:	$H_3C{-}C{\equiv}CH$	40	–	–	–	–	–	–	–	–	–
x:	CO	28	–	46	–	–	–	–	78	–	–
y:	$H_2C{=}O$	30	–	–	–	–	–	–	–	–	–
m:	CH_3OH	32	–	50	–	–	–	–	–	–	–
k:	CO_2	44	46	–	–	–	76	–	94	–	–
f:	HCOOH	46	–	–	–	–	78	–	96	–	–
e:	C_2H_5OH	–	–	–	–	–	–	–	–	–	–
ow:	[structure: O, 10, 14, HO, 11, Me 43, 13, 12]	114	–	–	–	142 −h 140	–	–	–	–	–
owx:	[structure: 14, O, O, 13, HO, 10, 9, 12, 11, Me 43]	142	−h 140	–	–	170 −h 168	–	–	–	–	–
a1:	[structure: O, 33, 30, 32, 28, 29, 31, O, 47 Me, 48 Me]	140	–	–	–	–	–	–	–	–	–
owxx:	[structure: 14, O, O, 13, HO, 10, 9, 12, 11, Me 43, O]	168	–	–	–	–	–	–	–	–	–
nx:	[structure: 3, 4, 2, 5, N, 7, O, 6]	111	–	129	–	–	143	155	161	–	–
fn:	[structure: 4, 3, OH, 5, 2, C, O, 6, N, H]	129	–	–	–	157 −h 155	161	–	179	–	–
fnx: 157	[structure: 4, 3, OH, 5, 2, C, 1, O, 6, N, 7, O]	157	−h 155	175 −h 173	–	–	189 −h 187	–	207 −h 205	–	–
fnxx: 157	[structure: 4, 3, OH, 5, 2, C, 1, O, 6, N, 7, O]	185	−h 183	203 −h 201	–	–	217 −h 215	–	235 −h 233	–	–
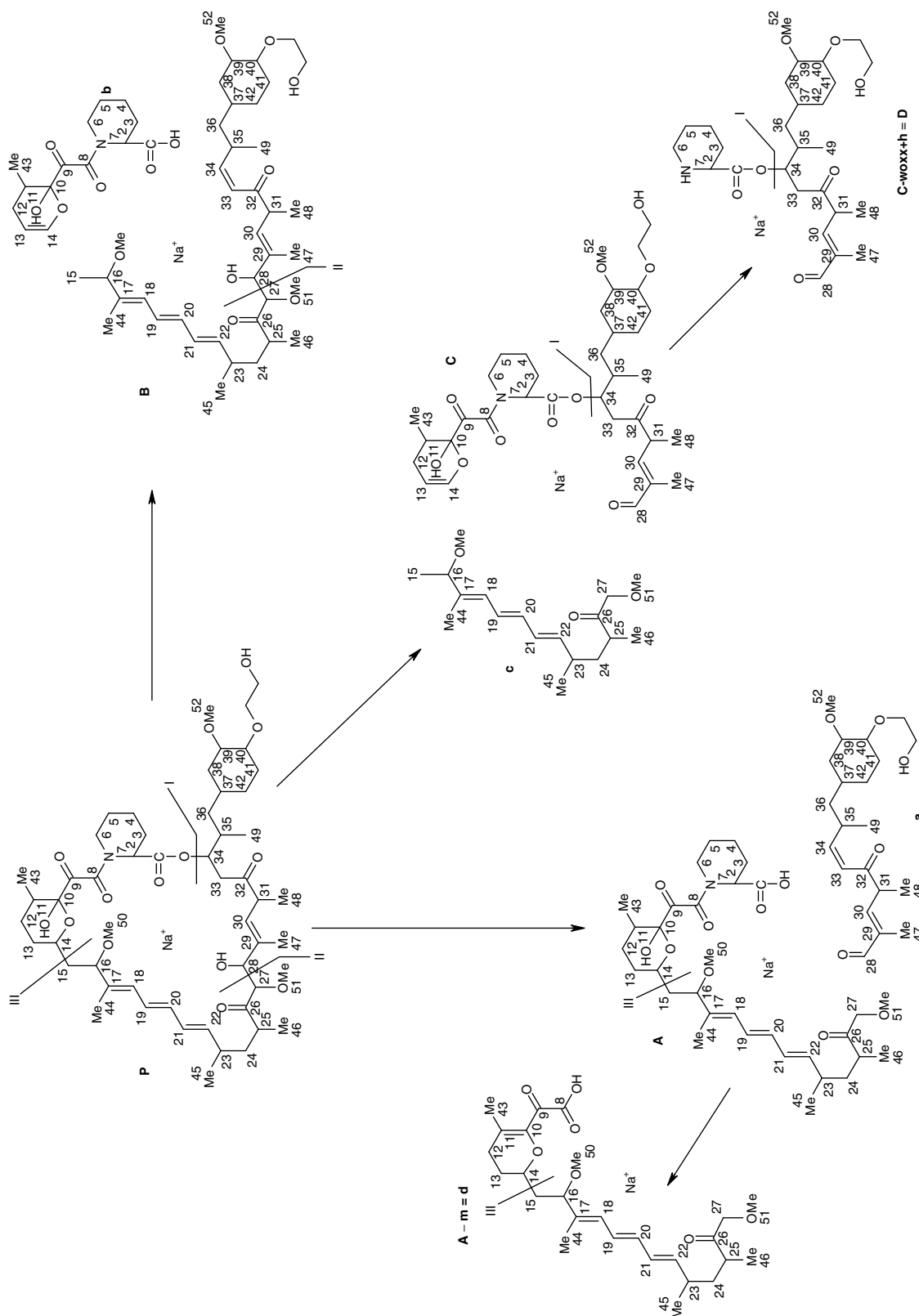
Figure 2. Initial steps in everolimus fragmentation. The parent molecule (P) dissociates into three main fragments (A), (B) and (C) and the corresponding cleaved fragments (a), (b) and (c). Further fragmentation of (C) leads to (D) and of (A) leads to (d). Some of these fragments are stabilized by the loss of methanol (m), leading to (B–m), (c–m), or (a–m). Sirolimus showed the same fragmentation pathway. Compared to everolimus, the *m/z* of the corresponding sirolimus fragments (P), (B), (C), (a) and (D) are 44 Da lower because of the 2-hydroxyethyl chain at position 40. As evaluated by MS^n experiments using an ion trap, all these fragments are further fragmented into smaller moieties.

However, in all the cases, sodium adduct $[M + Na]^+$ ions displayed signal intensities higher than that of the corresponding $[M + NH_4]^+$ ions. Adduct formation was primarily dependent on the cone voltage; $[M + Na]^+$ ions were formed almost exclusively at a cone voltage of 100 V, while $[M + NH_4]^+$ ions were predominant at lower cone voltages. In comparison, monitoring of negative electrospray-MS signals resulted in lower signal intensities and less detectable CID fragments. Different solvents or solvent pH also had a negative impact on ion signal

Table 2. Everolimus fragments (see also Supplementary Tables 1 and 2)

Mass	Formula	Notation	H/D Exp.	H/D theor.	Mass exp.	Mass error [ppm]	Comment
980.5711	$C_{53}H_{83}NO_{14}Na^+$	P-m	3	3	980.5750	+3.9	
962.5605	$C_{53}H_{81}NO_{13}Na^+$	P-w A-w					Can be derived from parent
952.5762	$C_{52}H_{83}NO_{13}Na^+$	P-x			952.5695	−7.0	980 − 28
950.5605	$C_{52}H_{81}NO_{13}Na^+$	P-y					980 − 30
948.5449	$C_{52}H_{79}NO_{13}Na^+$				948.5392	−6.0	
936.5813	$C_{52}H_{83}NO_{12}Na^+$	P-k					−a
934.5813	$C_{52}H_{81}NO_{12}Na^+$	P-f or P-e					980 − 46
930.5343	$C_{52}H_{77}NO_{12}Na^+$	P-mw			930.5288	−6.0	980 − 18 (w) − 32 (m)
851.4922	$C_{47}H_{72}O_{12}Na^+$	P-nxw					980 − 129 (−nx-w)
837.4765	$C_{46}H_{70}O_{12}Na^+$	P-kxm	2–3	3	837.4733	−3.8	
825.5129	$C_{46}H_{74}O_{11}Na^+$		3	3	825.5089	−4.8	
819.4659	$C_{46}H_{68}O_{11}Na^+$				819.4618	−5.0	
807.5023	$C_{46}H_{72}O_{10}Na^+$	P-knxw	2	2	807.4995	−3.5	
793.4867	$C_{45}H_{70}O_{10}Na^+$		2	2	793.4840	−3.4	= 980 − 155(knx) − 32(m)
775.4761	$C_{45}H_{68}O_9Na^+$		2	2	775.4746	−1.9	= 980 − 173 (k nx w) − 32 (m)
747.4812	$C_{44}H_{68}O_8Na^+$	P-knxwmx	1–2	2	747.4783	−3.9	= 980 − 205 (k nx w m) − 28 CO
686.3516	$C_{35}H_{53}NO_{11}Na^+$	$C = P − c$	2		686.3503	−1.9	
683.4499	$C_{39}H_{64}O_8Na^+$	$B = P − b$					This mass fragment ion is of very low intensity. = 980 − 297 (b)
651.4237	$C_{38}H_{60}O_7Na^+$	B-m	2	2	651.4244	+1.1	= 980 − 329 = 980 − 297 (b) − 32 (m)
614.3315	$C_{32}H_{49}NO_9Na^+$	$A = P-a$	2	2	614.3315	+1.6	= 980 − 366 (a)
596.3199	$C_{32}H_{47}NO_8Na^+$	A-w			596.3203	+0.6	= 980 − 366(a) − 18(w)
582.3043	$C_{31}H_{45}NO_8Na^+$	A-y	1–2	2	582.3058	+2.6	= 980 − 366 (a) − 32 (m)
570.3407	$C_{31}H_{49}NO_7Na^+$	A-k			570.3408	+0.2	= 980 − 366 (a) − 44 (k)
564.2937	$C_{31}H_{43}NO_7Na+$	A-f	0–1	1	564.2931	+0.2	= 980−366 (a) − 18 (w) − 32 (m)
546.3043	$C_{28}H_{45}NO_8Na^+$	B-owx			546.3048	+0.9	= 980−294 (c) − 140 (= 142 (owx) − h)
538.3145	$C_{30}H_{45}NO_6Na^+$	A-mk			538.3153	+1.6	= 980 − 366 (a) − 32 (m) − 44 (k)
518.2882	$C_{30}H_{41}NO_5Na^+$	A-mwf	–				**= 980**−366 (a) − 32 (m) − 18 (w) − 46 (f)
518.3094	$C_{27}H_{45}NO_7Na^+$	$D = P-d$	2	2	518.3035	+3.1	= 980 − 464 + 2 (d)
503.2621	$C_{26}H_{40}O_8Na^+$		1–2	2	503.2748	−5.1	= 980 − 366 (a) − 111 (nx)
485.2515	$C_{26}H_{38}O_7Na^+$	$D = A − fn = P − d$	1	1	485.2541	+5.3	= 980 − 366 (a) − 111 (nx) − 18 (w)
471.2359	$C_{25}H_{36}O_7Na^+$	A-nxm	1–2	2	471.2381	−4.7	= 111 (nx) − 32 (m)
459.2723	$C_{25}H_{40}O_6Na^+$	A-fnx-h			459.2735	+2.7	= 980 − 366 (a) = 155 (= 157 − 2 (fnx-h))
453.2253	$C_{25}H_{34}O_6Na^+$	A-nxwm	0–1	1	453.2281	−6.2	= 980 − 366 (a) − 18 (w) − 32 (m)
441.2253	$C_{25}H_{38}O_5Na^+$	A-fnxw-h	0–1	0	441.2595	+5.0	= 980 − 366 (a) − 155 (fnx-h) − 18 (w)
427.2460	$C_{24}H_{36}O_5Na^+$	A-fnxm-h	2	2	427.2483	+5.3	= 980 − 366 (a) − 32 (m) − 155 (fnx-h)
425.2304	$C_{24}H_{34}O_5Na^+$	A-fnxm			425.2306	0.5	As above − h_2
409.2355	$C_{24}H_{34}O_4Na^+$	A-fnxmw-h	0–1	0	409.2381	+6.4	= 366 (a) − 18 (w) − 32 (m) − 155 (fnx-h)
389.2304	$C_{21}H_{34}O_5Na^+$	$A = P − A$	0–1	1	389.2356	−13.4	= 980 − 614 (A) + 23 (Na$^+$)
381.2406	$C_{23}H_{34}O_3Na^+$	A-fnxxmw-h	0	0	381.2418	+3.2	= 980 − 366 (a) − 18 (w) − 32 (m) − 183 (= 185 (fnxx) − 2 (h))
320.1110	$C_{14}H_{19}NO_6Na^+$	$B = P − b$	0–1	2	320.1114	−1.2	The mass shift should be of 2 deuterium in this case = 980 − 660 (B)
317.2093	$C_{18}H_{30}O_3Na^+$	$C = P − c$					= 980 − 663 (C)
311.1987	$C_{19}H_{28}O_2Na^+$	a-me	0	0	311.1983	−1.3	= 980 − 591 (A) − 32 (m) − 46 (e)
285.1831	$C_{17}H_{26}O_2Na^+$	c-m	0–1	0	285.1775	−3.3	= 980 − 663 (C) − 32 (m)
276.1212	$C_{13}H_{19}NO_4Na^+$	b-k					= 980 − 660 (A) − 44 (k)
249.0739	$C_{11}H_{14}O_5Na^+$	meox					

Table 2. (*Continued*)

Mass	Formula	Notation	H/D Exp.	H/D theor.	Mass exp.	Mass error [ppm]	Comment
245.1518	$C_{14}H_{22}O_2Na^+$	c-meCH$_2$	0				
209.1154	$C_{10}H_{18}O_3Na^+$	A1	0–1	1	209.1234	+1.5	
209.0426	$C_8H_{10}O_5Na^+$	–	0–1	2	209.0424	−0.9	
205.1204	$C_{10}H_{14}O_3Na^+$	meox	0	0	205.1200	−2.2	
203.1048	$C_{11}H_{16}O_2Na^+$	A2					
173.0579	$C_9H_{10}O_2Na^+$	eox					
165.0528	$C_7H_{10}O_3Na^+$	–					= 980 − 660 (B) − 155 (fnx-h)
152.0688	$C_6H_{11}NO_2Na^+$	–					

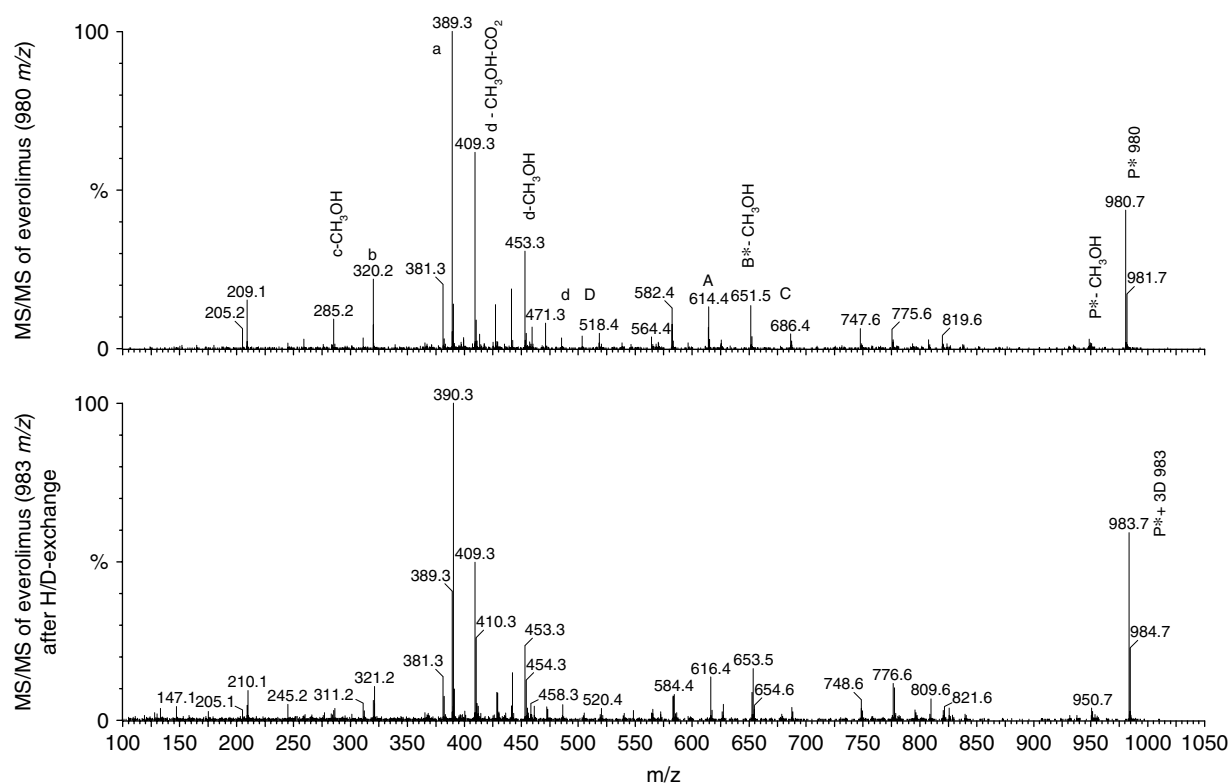Abbreviations: exp., experimental; theor., theoretical; H/D, number of exchangeable hydrogen atoms.

Figure 3. LC-tandem mass spectra of 980/983 *m/z* (everolimus, [M + Na]$^+$) before and after H/D exchange. To facilitate visual inspection, the mass labels are rounded off to one digit, while original data had mass accuracies of four decimals.

intensities. Ion trap experiments were performed on an LCQ instrument (Thermo-Finnigan, San Jose, CA, USA).

Hydrogen/Deuterium (H/D) exchange

For the H/D exchange experiments, water in the mobile phase of the HPLC system was replaced with D$_2$O and methanol with MeOD. The retention time of everolimus on the column was sufficient for the replacement of hydrogen by deuterium, with an average exchange rate of H/D at 96%.

Notation

In order to better understand the complex fragmentation pathways of everolimus, a special mass fragment ion notation was introduced. The upper case letters (**A**), (**B**), (**C**) and (**D**) were assigned to the four major everolimus fragments, while the lower case letters (**a**), (**b**), (**c**) and (**d**) were

assigned to the corresponding cleaved fragments (Fig. 2). Each main fragment created a large number of additional subfragments due to neutral losses. However, while a total of 69 different neutral losses were identified, only 18 of those and their combinations were considered important (Table 1). For example, the loss of methanol was symbolized by 'm' and the loss of water was symbolized by 'w'. Accordingly, the combined loss of methanol and water was indicated by 'mw', having a total loss of 50 Da (= 32 + 18 Da).

The mass shift for each fragment can be interpreted using Table 1. The mass values in Table 1 show the most common combinations of neutral losses for the given fragments. With this notation in place and the transfer of the high-resolution mass spectral data into an Excel table by converting the data into a centroid mass list, it was possible to identify the important fragments within a measurement easily. With
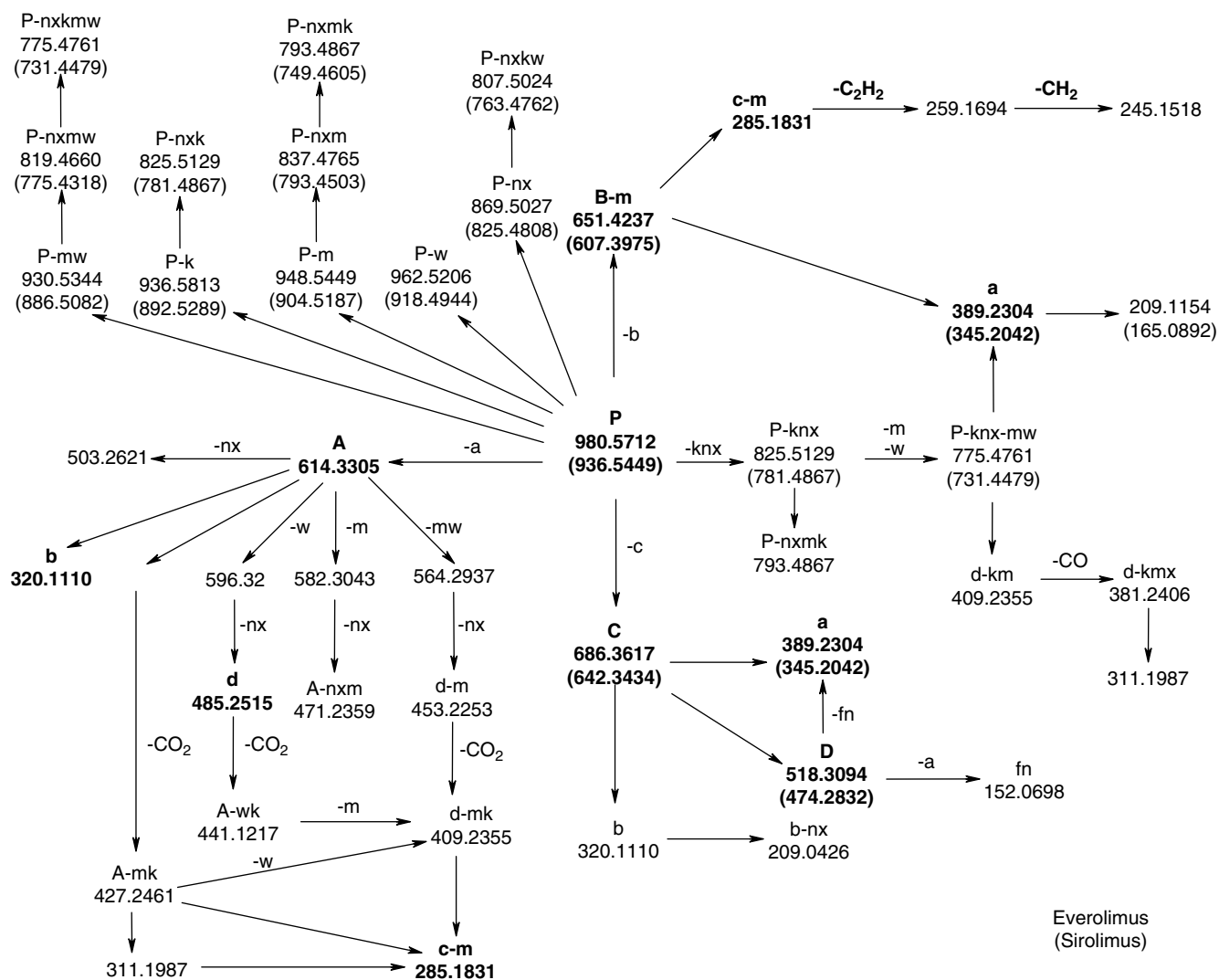
Figure 4. Main fragmentation pathways of everolimus and sirolimus. All *m/z* values (calculated exact masses) shown are those of the sodium adducts. Sirolimus data is in brackets. If there are no brackets, everolimus and sirolimus formed the same fragment. The annotations is described in Table 1. Fragment structures are shown in Supplementary Tables 1 and 2.

RESULTS AND DISCUSSION

the knowledge of the reaction pathways and the neutral losses, we could simulate the fragmentation patterns for all structural isomers and metabolites. In this manner, it was possible to create 448 different theoretical fragmentation pathways from the combinations of the 56 existing different neutral losses and the main eight fragments of everolimus, given in Fig. 2. All neutral losses as a combination of common losses, like water or CO, and the specific neutral losses of everolimus (or sirolimus) are listed in Table 1. Only the main observed neutral losses are included in the table to keep it readable.

RESULTS AND DISCUSSION

In comparison to the structurally related sirolimus (913.5551 Da), the ionization of everolimus was 5-fold less efficient. In addition, sirolimus yielded fragments that had significantly higher ion signal intensities than everolimus. It was found that the presence of sodium and also potassium ions gave relatively strong intensities. This can be explained by a strong affinity of these ions to the macrolides. This is even

more interesting considering that no sodium salts were added. The small amounts of sodium ions in the solvents obviously provided sufficient sodium ions for the ionization. By adjusting the cone voltage, formation of $[M + NH_4]^+$ could be suppressed. In contrast to $[M + Na]^+$, $[M + NH_4]^+$ ions did not give detailed fragmentation patterns.

Small quantities of detectable K^+ ions produced $[M + K]^+$, which resulted in a mass difference of 16 Da ($= 39 - 23$ Da) with respect to $[M + Na]^+$. It is important to have this knowledge for the structural elucidation of metabolites since such K^+ adducts could be incorrectly interpreted as an additional oxygen atom in the fragments of low resolution data and unnecessarily complicate high resolution data. Therefore, the analytes were loaded into an online precolumn and washed with 100 μl of water/methanol (95/5; v/v) prior to LC/MS analysis. This step completely eliminated the formation of potassium adducts.

The difference between everolimus and sirolimus lies not only in the structural addition of the hydroxyethyl group, but also in their differing pharmacological behaviors. One important issue is whether sirolimus is formed during

the biotransformation of everolimus (by a loss of 44 Da). Indeed, an everolimus derivative with a loss of 44 Da was observed; however, it need not necessarily be sirolimus, since alternatively a mass loss of 44 Da is possible with the loss of CO_2 from position 1 of everolimus. Using low resolution mass spectrometry, further fragmentation of the 936 Da fragment by CID made it possible to differentiate between the two fragments. In the case, where fragment (**a**) lost 44 Da, the hydroxyethyl group was cleaved off. In the case where fragment (**b**) lost 44 Da, CO_2 was cleaved off. This fragmentation behavior was observed with everolimus and sirolimus in the common mass fragment $m/z = 775.4761$. This fragment can be explained either as P-knxwm for everolimus (Table 2 and Fig. 4) or P-fnm for sirolimus (Table 2 at $m/z = 819 - 44$).

The complex fragmentation patterns of everolimus along with the existence of the ester hydrolysis products (preseco-everolimus and seco-everolimus) made it imperative that the best separation techniques for all analytes were used. The overlap of chromatographic peaks made the interpretation of mass spectra nearly impossible. It was critical that the LC system provided the highest resolution and sensitivity for the mass spectrometer. As a result, a microbore HPLC system was used, which provided peaks with a half-width of 9 s or less.

The interpretation of the measured mass spectra became more reliable after combining the QTOF mass spectra with spectra from the LCQ ion trap. Both mass spectrometers had unique electrospray systems and produced different spectra. However, all molecular fragments were found on both the instruments, while the individual fragment ion intensities varied. To produce the most reliable spectra, MS^3 analyses were performed on the instrument that produced a higher yield of the corresponding MS^2 signal.

Hydrogen/Deuterium exchange

In electrospray mass spectrometry, hydrogen/deuterium exchange is a commonly used method for structure elucidation for confirming the presence of active hydrogens in organic compounds (i.e. hydrogens attached to heteroatoms O, N, and S).[11-14] After switching the mobile phases of the HPLC system to D_2O and CH_3OD and extensive flushing with these deuterated solvents, an exchange rate of greater than 96% was achieved. Under soft ESI conditions (low cone voltages), the shift of the parent ion displayed the number of active hydrogen atoms. Both everolimus and sirolimus contain three hydroxyl groups, which reacted to form –OD and resulted in a mass shift of 3 mass units (Fig. 3). Again, it must be noted that all molecules were ionized as $[M + Na]^+$-ions. In most cases, after fragmentation of the deuterated parent ions under low CID conditions, the predicted mass shift was observed for the individual fragments. However, when molecular fragments are intentionally excited to produce conformational changes or fragmentations, the results could potentially be misinterpreted because of the deuterium atom scrambling into unexpected positions in some cases. For example, with everolimus, an additional deuterium additive was observed at position 27, after the carbon bond between 28 and 27 was broken by CID (i.e. fragment A-fnxm-h,

$m/z = 427.2460$). Another fragment (b, $m/z = 320.1110$) was predicted to have a mass shift of 2 Da, yet only a shift of 0 to 1 Da was observed. This example shows that H/D exchange data of fragments are useful to confirm a given structure, but should not be used to predict new structures of everolimus metabolites. Overall, it can be seen that there was a significant agreement between the larger mass everolimus fragments. Only a few of the smaller fragments, which were the result of several fragmentation steps (excited fragments), showed incorrect data by one additional mass shift. Although CID typically only provides additional confirmation of the proposed structure, in our case, CID aided in the structural elucidation of everolimus itself.

The H/D exchange experiments clearly showed the number of hydroxyl groups. This is the only experiment that distinguished between an epoxide and a hydroxyl group as a result of two possible biotransformation reactions. Because epoxy metabolites of sirolimus and everolimus have been proposed,[15,16] this experiment was important for determining the correct structures of all metabolites.

Accurate mass determination

One of the most critical tools for the verification of everolimus fragment structures was the determination of the accurate mass of each fragment.[17-19] The QTOF mass spectrometer used in our study allowed determination of the elemental composition of product ions with an accuracy better than 5 ppm when using the residual precursor ion as a single-point internal calibrant.[20] We realize that more modern time-of-flight mass spectrometers as well as other high-resolution mass spectrometry technologies, such as orbitrap and Fourier transformation-MS, allow for better resolutions than those reported here. However, since for everolimus fragments only a limited number of structural alternatives were possible, the resolution achieved was in most cases more than sufficient to demonstrate which of the structural alternatives was correct. In addition, we used MS ion trap data and H/D exchange experiments to further support the everolimus fragment structures. We were also fully aware of the fact that additional mass accuracy errors may occur in the case of unresolved interferences.[21] Thus, we used an efficient LC procedure to separate everolimus from potential interferences such as the seco-everolimus degradation products. Only high-resolution spectra of MS/MS experiments were used for structural elucidation. There was never any indication that interferences negatively affected the results of this study.

It is reasonable to assume that with the achieved mass accuracy, a reliable determination of the elemental composition was feasible. However, QTOF data became incorrect if one of the mass peaks had very high signal intensity. This was because of the given delay of its detector system (Time-to-Digital-Converter, TDC dead time). This effect was observed in fragment (a) with a mass of 389.2304 (Table 2) and a mass error of 13.4 ppm, while all other spectral peaks had mass errors below 6 ppm. An interesting example of the power of accurate mass determinations can be seen in the fragment 209.0426 Da ($C_8H_{10}O_5Na$) (notation: b−nx). This fragment was formed by the fragmentation pathway P → C → b → b-nx, while the fragment 209.1154 Da

produced a seven ring system by the alternate pathway $P \rightarrow C \rightarrow a \rightarrow C_{10}H_{18}O_3Na$. Because this fragment (b-nx) contained the 2-hydroxyethyl chain, it was not observed in sirolimus when the mass fragment at 209.1154 Da was present. Table 2 shows good agreement with the measured elemental composition for nearly all proposed fragment structures. With such a large number of different fragments, it was possible to select different lock masses for the single-point calibration of the measured spectra. This offered the opportunity to cross-validate all structures. Table 2 presents the results of several MS/MS experiments with different lock-masses; however, this resulted only minor changes in the values listed in this table and thus the data are not shown.

Fragmentation pathways

Everolimus and sirolimus were both fragmented along the same pathways. The only difference observed was in the individual fragment intensities. Figure 2 gives an overview of the first fragmentation steps.

As demonstrated for everolimus, the $[M + Na]^+$ ($m/z = 980.5711$) was split at three different positions, including binding position I, II and III, resulting in six main fragments of $m/z = 285.1831$ (C-m), 320.1111 (**b**), and 389.2304 (**a**) as well as 614.3315 (A), 651.4237 (B-m) and 686.3516 (**C**), (measured values given) as shown in Fig. 2 and Supplementary Table 1.

Three of the above six fragment ions 285.1831 (C-m), 591.3417 (A-m) and 651.4237 Da (B-m)) had lost a methoxy group, as characterized by the loss of methanol (-32.026 Da). The mass difference before and after H/D exchange was 3 Da indicating that the molecules contained a total of three exchangeable hydrogen atoms. Most of the proposed structures were confirmed by accurate mass measurement and were within a range of -5 to $+5$ ppm.

Because of the size of everolimus and the large number of fragments, Fig. 4 shows only the theoretical masses and notations of selected fragments. Table 2 and Supplementary Tables 1 and 2 contain additional information for each fragment.

CONCLUSIONS

In our study, the key to identifying the complex fragmentation pattern of everolimus was through the combined use of a quadrupole time-of-flight mass spectrometer (QTOF) and an ion trap instrument for MS^n experiments. The reliability of our data is verified by the fact that two laboratories (Basel and San Francisco) independently produced exactly the same results. The fact that the two types of instruments have different collision cells for fragmentation results in different intensities of the same fragment ion. In this way, it was possible to determine even very weak fragment ions on one instrument, while it was intense on the other one.

Because of the lack of detailed structural information of everolimus fragments, previous attempts to identify everolimus structures using LC/MS were not only of limited success,[22] but also led to incorrect conclusions.[15,16] We would like to emphasize again that the H/D experiments are critical to prove the number of hydroxylations, and clearly excluded epoxy metabolites of sirolimus and everolimus,[15,16] which have been proposed based on nonvalidated hypothetical fragmentation patterns.

Supplementary material

Supplementary electronic material for this paper is available in Wiley InterScience at: http://www.interscience.wiley.com/jpages/1076-5174/suppmat/.

REFERENCES

1. Sedrani R, Cottens S, Kallen J, Schuler W. Chemical modification of rapamycin: the discovery of SDZ RAD. *Transplantation Proceedings* 1998; **30**: 2192.
2. Schuler W, Sedrani R, Cottens S, Haberlin B, Schulz M, Schuurman HJ, Zenke G, Zerwes HG, Schreier MH. SDZ RAD, a new rapamycin derivative: pharmacological properties *in vitro* and *in vivo*. *Transplantation* 1997; **64**: 36.
3. Schuurman HJ, Cottens S, Fuchs S, Joergensen J, Meerloo T, Sedrani R, Tanner M, Zenke G, Schuler W. SDZ RAD, a new rapamycin derivative: Synergism with cyclosporine. *Transplantation* 1997; **64**: 32.
4. Gummert JF, Ikonen T, Morris RE. Newer immunosuppressive drugs: a review. *Journal of the American Society of Nephrology* 1999; **10**: 1366.
5. Nashan B. Early clinical experience with a novel rapamycin derivative. *Therapeutic Drug Monitoring* 2002; **24**: 53.
6. Hallensleben K, Raida M, Habermehl G. Identification of a new metabolite of macrolide immunosuppressants, like rapamycin and SDZ-RAD, using high-performance liquid chromatography and electrospray tandem mass spectrometry. *Journal of the American Society for Mass Spectrometry* 2000; **11**: 516.
7. Nickmilder MJ, Latinne D, de Houx JP, Verbeeck RK, Lhoëst GJ. Isolation and identification of a C39 demethylated metabolite from pig liver microsomes and evaluation of its immunosuppressive activity. *Clinical Chemistry* 1998; **44**: 532.
8. Nickmilder MJ, Latinne D, Verbeeck RK, Janssens W, Svoboda D, Lhoëst GJ. Isolation and identification of new rapamycin dihydrodiol metabolites from dexamethasone-induced rat liver microsomes. *Xenobiotica* 1997; **27**: 869.
9. Streit F, Christians U, Schiebel HM, Meyer A, Sewing KF. Structural identification of four metabolites of the macrolide immunosuppressant sirolimus after in vitro metabolism by electrospray-MS/MS. *Drug Metabolism and Disposition* 1996; **24**: 1272.
10. IUPAC Nomenclature of Organic Chemistry. *A Guide to IUPAC Nomenclature of Organic Components (Recommendations 1993)*. Blackwell Scientific Publications: Boston 1993.
11. Hopfgartner G, Chernushevich IV, Covey T, Plomley JB, Bonner R. Exact mass measurement of product ions for the structural elucidation of drug metabolites with a tandem quadrupole orthogonal-acceleration time-of-flight mass spectrometer. *Journal of the American Society for Mass Spectrometry* 1999; **10**: 1305.
12. Pfeifer T, Tuerk J, Fuchs R. Structural characterization of sulfadiazine metabolites using H/D exchange combined with various MS/MS experiments. *Journal of the American Society for Mass Spectrometry* 2005; **16**: 1687.
13. Reed DR, Kass SR. Hydrogen-Deuterium exchange at non-labile sites: a new reaction facet with broad implications for structural and dynamic determinations. *Journal of the American Society for Mass Spectrometry* 2001; **12**: 1163.
14. Palmer ME, Tetler LW, Wilson ID. Hydrogen/deuterium exchange using a coaxial sheath-flow interface for capillary

electrophoresis/mass spectrometry. *Rapid Communications in Mass Spectrometry* 2000; **14**: 808.

15. Lhoëst GJ, Gougnard TYR, Verbeeck RK, Maton N, Dehoux JP, Wallemacq P, Schüler W, Latinne D. Isolation from pig liver microsomes, identification by tandem mass spectrometry and in vitro immunosuppressive activity of an SDZ-RAD 17,18,19,20,21,22-tris-epoxide. *Journal of Mass Spectrometry* 2000; **35**: 454.

16. Lhoëst GJ, Hertsens R, Verbeeck RK, Maton N, Wallemacq P, Dehoux JP, Latinne D. In vitro immunosuppressive activity of tacrolimus dihydrodiol precursors obtained by chemical oxidation and identification of a new metabolite of SDZ-RAD by electrospray and electrospray-linked scan mass spectrometry. *Journal of Mass Spectrometry* 2001; **36**: 889.

17. Bristow AWT. Accurate mass measurement for the determination of elemental formula – a tutorial. *Mass Spectrometry Reviews* 2006; **25**: 99.

18. Cottee F, Haskins N, Bryant D, Eckers C, Monte S. The use of accurate mass measurement by orthogonal time-of-flight mass spectrometry in pharmaceuticals research. *European Journal of Mass Spectrometry* 2000; **6**: 219.

19. Lopes NP, Stark CBW, Hong H, Gates PJ, Stounton J. Fragmentation studies on monensin A and B by accurate mass electrospray tandem mass spectrometry. *Rapid Communications in Mass Spectrometry* 2002; **16**: 414.

20. Köfeler HC, Gross ML. Correction of accurate mass measurement for target compound verification by quadrupole time-of-flight mass spectrometry. *Journal of the American Society for Mass Spectrometry* 2006; **16**: 406.

21. Blom KF. Utility of peak shape analyses in determining unresolved interferences in exact mass measurements at low resolution. *Journal of the American Society for Mass Spectrometry* 1998; **9**: 789.

22. Vidal C, Kirchner GI, Sewing K-Fr. Structural elucidation by electrospray mass spectrometry: an approach to the in vitro metabolism of the macrolide immunosuppressant SDZ RAD. *Journal of the American Society for Mass Spectrometry* 1998; **9**: 1267.